Mon. Not. R. Astron. Soc. **000**, 000–000 (0000) Printed 5 February 2008 (MN LATEX style file v1.4)

Short timescale variability in the Faint Sky Variability Survey

L. Morales-Rueda[1], P. J. Groot[1], T. Augusteijn[2], G. Nelemans[1], P. M. Vreeswijk[3,4] E. J. M. van den Besselaar[1]

[1]*IMAPP, Department of Astrophysics, Radboud University Nijmegen, P.O. Box 9010, 6500 GL Nijmegen, The Netherlands. E-mail: lmr@astro.ru.nl, pgroot@astro.ru.nl, nelemans@astro.ru.nl, besselaar@astro.ru.nl*

[2]*Nordic Optical Telescope, Apartado 474, E-38700 Santa Cruz de La Palma, Spain. E-mail: tau@not.iac.es*

[3]*European Southern Observatory, Alonso de Córdova 3107, Vitacura, Casilla 19001, Santiago 19, Chile. E-mail: pvreeswi@eso.org*

[4]*Departamento de Astronomía, Universidad de Chile, Casilla 36-D, Santiago, Chile.*

Accepted ... Received ...; in original form ...

ABSTRACT

We present the V band variability analysis of the point sources in the Faint Sky Variability Survey on time scales from 24 minutes to tens of days. We find that about one percent of the point sources down to V = 24 are variables. We discuss the variability detection probabilities for each field depending on field sampling, amplitude and timescale of the variability. The combination of colour and variability information allows us to explore the fraction of variable sources for different spectral types. We find that about 50 percent of the variables show variability timescales shorter than 6 hours. The total number of variables is dominated by main sequence sources. The distribution of variables with spectral type is fairly constant along the main sequence, with 1 per cent of the sources being variable, except at the blue end of the main sequence, between spectral types F0–F5, where the fraction of variable sources increases to about 2 percent. For bluer sources, above the main sequence, this percentage increases to about 3.5. We find that the combination of the sampling and the number of observations allows us to determine the variability timescales and amplitudes for a maximum of 40 percent of the variables found. About a third of the total number of short timescale variables found in the survey were not detected in either B or/and I. These show a similar variability timescale distribution to that found for the variables detected in all three bands.

Key words: surveys – methods: data analysis – stars: general – stars: statistics – stars: variables: general

1 INTRODUCTION

There is a wide range of photometrically variable systems in the universe. The range of timescales on which these systems vary is as wide as the physical processes that produce their variability. For example we have intrinsically variable stars, where the variability is caused by changes in their internal structure or atmosphere that vary with timescales of minutes to years (Brown & Gilliland 1994). Other stars show variability because they rotate and their surface is inhomogeneous, e.g. because of star spots, (Brinkworth et al. 2005), or because they form part of a binary or multiple system and their revolution around the centre of mass of the system results in changes on the detected flux due to the changing aspect of a non-isotropically emitting surface or eclipses. This is also the case for planets orbiting stars. The timescale of the variability in this case is dictated by the orbital parameters of the system and can range from seconds to years. Near Earth Objects (NEOs), such as asteroids, also show variability as they rotate and are non-spherical. We find photometric variability in extragalactic objects as well, such as quasars, where the variability is probably the result of material being accreted by the central engine, or "one of" systems such as gamma ray bursts (GRB) or supernovae (SNe) where the variability is produced by intrinsic changes in the structure of an astronomical object that take place only once.

The study of variability provides important information about the physical nature of the variable objects, leads to the discovery of new classes of objects, helps to study the physical structure of stars, e.g. pulsating stars, allows us to obtain information on galactic structure through the use of variables such as RR Lyrae as standard candles, and is the key to determining extra-galactic distances through the use

of standard candles such as Cepheids and supernovae Type Ia.

Most of our knowledge of variability is based on the study of apparently bright sources, which naturally selects members of *intrinsically* bright populations. At present little is known about variability of intrinsically fainter populations because in bright samples they are lacking altogether or are only represented by a few members. The Faint Sky Variability Survey (FSVS; Groot et al. (2003)) was designed to account for this deficit by studying two unexplored regions of the variability space: the short timescale variability region (down to tens of minutes) and the intrinsically faint variable sources (down to V = 24 mag) at mid and high Galactic latitudes. The FSVS also contains colour information for all targets, giving us the option of positioning objects in the colour-colour diagram as well as finding the variability timescales and amplitudes that characterise them. The main aims of the FSVS are thus to obtain a map of a region of the Galaxy ($\sim$21 deg^2) in variability and colour space, to determine the population density of the different variable objects that reside in the Galaxy and to find the photometric signature of up-to-now unknown intrinsically faint variable populations. In this paper we explore these three goals.

There are other surveys that study the variable optical sky, each emphasising one aspect or one particular region of this parameter space. The timescales sampled, depth and sky coverage of different variability surveys varies depending on the astronomical objects they are designed to study. For example, with a brightness limit similar to the FSVS, Street et al. (2005) study the variability around an open cluster with timescales longer than a few hours, and Ramsay & Hakala (2005) study the rapid variability (down to 2 minutes) of objects as faint as V$\sim$22.5. Of great interest is the Deep Lens Survey (DLS) that, in a similar way to the FSVS, combines colour and variability information and explores similar variability timescales (Becker et al. 2004). Becker et al. (2004) also provide a comprehensive review of past and on-going variability surveys.

The future of optical variability surveys looks quite promising with the advent of large aperture telescopes such as the Large-aperture Synoptic Survey 8.4 m Telescope (Tyson 2002), the 4 m telescope VISTA and the 2.5 m VLT Survey Telescope.

2 OBSERVATIONS

The full Faint Sky Variability Survey (FSVS) data set consists of 78 Wide Field Camera (WFC) fields taken with the Isaac Newton telescope (INT) at La Palma. The FSVS covers an area in the sky of $\sim$21 deg^2 located at mid and high Galactic latitudes ($-40< b <-21$, $15< b <50$, $89< b <90$). The WFC is a moisac of four 2kx4k CCDs. For each field, we took one set of B, I and V band observations on a given photometric night. Photometric variability observations were taken with the V filter on several consecutive nights. On average, fields were observed 10 – 20 times within one week in the V band. Exposure times were 10 min with a dead time between observations of 2 min. This observing pattern allows us to sample periodicity timescales from 2×(observing time + dead time) (i.e. 24 min) to twice the maximum time separation of observations (which ranges from 3 days to 13 days). See for more details Groot et al. (2003).

All fields were re-observed years later to determine proper motions. In this paper we concentrate on the shorter timescale variability (from 0.4 hours to a few days) of the targets and we do not include those observations.

Of the 78 fields, 10 were only observed in the V band

Table 1. Journal of observations. The number of V band observations taken for each field, not counting those taken about a year later for proper motion studies, as well as the maximum time interval covered in days, Δt, are given. For field 48, the two V band measurements were taken more than a year apart. For field 51, two measurements were lost in one of the CCDs. The fraction of variable sources (FV) x100 per field found using the χ^2 test is also given. This will be discussed in detail in Sections 3.1 and 4.1. Notice that the fraction of variables found in fields 36, and 48, is very high compared to the rest of the fields. These fields were only observed in 2 occasions so their variability χ^2 was calculated based only on 2 points. This is also the case for fields 35, and 41 to 45 but they do not show a fraction of variables as large. These 6 fields contain about twice the number of stars compared to fields 36 and 48.

Field	V obs	Δt	FV	Field	V obs	Δt	FV
01	10	5.07	0.59	40	9	3.07	3.44
02	11	5.07	1.04	41	2	0.06	3.22
03	13	5.11	0.21	42	2	0.91	3.91
04	12	3.04	1.19	43	2	0.03	1.62
05	12	3.09	0.55	44	2	0.03	2.05
06	10	3.11	0.74	45	2	0.03	1.90
07	10	5.99	0.48	46	19	4.18	1.06
08	11	5.07	0.09	47	5	6.97	4.20
09	10	5.02	0.79	48	2	-	8.60
10	10	3.02	0.09	49	3	5.94	5.26
11	7	3.04	0.23	50	3	6.07	3.75
12	8	3.07	0.31	51	5,3	5.92	2.09
13	9	5.06	0.77	52	26	5.17	0.80
14	10	5.03	0.54	53	20	6.10	0.24
15	8	3.03	0.55	54	20	6.01	0.15
16	12	3.06	0.51	55	20	5.98	1.11
17	8	3.09	0.64	56	19	4.18	0.37
18	9	5.06	0.67	57	18	5.24	1.30
19	11	4.02	0.35	58	15	4.18	0.70
20	11	4.04	0.11	59	20	5.12	0.60
21	11	4.07	0.74	60	22	4.16	1.93
22	11	4.05	2.73	61	20	4.09	0.47
23	11	4.08	3.06	62	19	4.06	1.95
24	10	4.11	1.62	63	22	6.09	0.52
25	30	6.12	0.06	64	22	6.06	0.43
26	29	5.00	0.58	65	20	6.03	0.40
27	14	6.01	0.25	66	21	6.00	0.41
28	14	5.99	0.66	68	28	12.07	1.11
29	14	6.02	0.45	69	29	13.00	1.50
30	16	4.99	1.60	70	24	6.03	0.88
31	16	4.99	0.87	71	27	6.00	1.04
32	16	4.99	0.36	72	26	6.11	0.50
33	18	6.10	0.18	73	27	6.09	0.66
34	17	6.07	0.42	74	26	6.05	0.23
35	2	0.03	1.83	75	25	6.00	0.21
36	2	0.97	13.68	76	33	7.03	0.37
37	10	4.08	0.35	77	33	7.06	0.48
38	9	4.05	0.73	78	33	7.15	0.48
39	9	3.09	0.77	79	31	7.15	0.28

on two or three occasions due to bad weather, making it impossible to use these for precise variability studies. We also encountered data acquisition/reduction problems in several occasions which resulted in parts of fields being lost. Initially 79 fields were defined but one, 67, was never observed. For data handling consistency we have kept the original numbering.

A complimentary analysis on the variability at short and long timescales (including year-long timescales) of the FSVS has been carried out by Huber et al. (2006). They make use of a variability test similar to that described in Section 3.1 to find signatures of the presence of variability with some indication of its timescale and amplitude. By using the yearly re-observations they find a variability fraction of 5 to 8 percent in two survey regions. This number is larger than that found in Section 4.1 due to several factors: in our analysis we are only considering short period variables and thus do not make use of the yearly re-observations, we determine the variability fraction using the entire area of the survey instead of two separate regions, and we use a reduced weighted χ^2 to establish variability instead of the reduced un-weighted χ^2 found in the public release FSVS data products. Most of the variable sources found by Huber et al. (2006) are long period variables classified as such thanks to the V brightness of the re-observation a year later. The number of possible periodicities in the data when the sampling is sparse and the time span long is very large and their analysis is devised to find possible variable systems more than to find their actual variability timescale and amplitude, which is one of the main goals of the work presented here.

Table 1 gives a list of the number of times each field was observed in V and the maximum time span of the data in each case. In summary, we have photometric data that can be used for variability analysis for $\sim$17.5 deg^2 out of the 21 deg^2 that constitute the FSVS. For $\sim$9.2 deg^2 the number of measurements is equal or more than 15 whereas for the other $\sim$8.3 deg^2 the number is between 5 and 15. This makes a difference in the accuracy with which we can measure the variability timescale of each object.

The methods used to study the variability in the data are presented in Section 3. The results from the variability analysis are discussed in the different subsections of Section 4. In this paper we carry out a full variability study for point sources that have not only more than 4 V band measurements taken over a two week baseline, but also positive detections in the B and I bands. Possible extreme colour systems are discussed in detail in Section 4.7.

2.1 Data quality checks

We carried out several tests to check the quality of the photometry. These included plotting several quantities obtained from the data to check for anomalies. We explored how the number of detected point sources changed with epoch for each field, the average point source V magnitude per epoch per field and the ratio between the point source mean magnitude and the limiting magnitude for each measurement.

We identified several fields that showed anomalies, such as field 31 CCD 4, in which one of the observations (number 14) resulted in V band magnitudes that were lower than the rest by 2 magnitudes. We found that the best way to identify these anomalies consisted of plotting the V band magnitudes for each point source detected in each field versus its error, for each observation. An example of this test is shown in Fig. 1 where the point sources found in Field 31 CCD 4 on four different epochs are plotted. Each panel presents the test for one observation. The average V band magnitude (Vave) for all point sources and the limiting magnitude (Vlim) for each image is also given. When the field was observed through thin clouds (e.g. epoch 13) the values of Vlim and Vave decrease but the shape of the curve does not change. On the other hand if something went wrong with the image or the data reduction we expect the shape of the curve to change (e.g. epoch 14) giving us an indication that we should be wary of this V point when doing our variability searches. We could not trace the reason for the anomaly found in epoch 14 of field 31 and just discarded this data point.

We also carried out visual inspection of the raw unfolded lightcurves for all the variable point sources to identify possible problematic photometry points and when confirmed these points were thrown out.

3 VARIABILITY ANALYSIS METHODS

3.1 The variability χ^2 test

Groot et al. (2003) determine the variability of a given point source in the FSVS by calculating the reduced χ^2 value of the object's individual brightness measurements with respect to its weighted mean brightness value. An object is tagged as variable if its reduced χ^2 is above the 5-σ level. This definition will be used in Sect. 4.1 to determine the fraction of variable objects in the survey. Because we have colour information for the majority of the objects, we can determine this ratio for different types of systems.

3.2 The floating mean periodogram

If we not only want to know whether an object is variable or not, but also what the timescale and amplitude of its variability are, and thus what type of object it might be, we need to use more refined methods to determine its variability. Because of the relatively small number of V band observations (between 2 and 33 depending on the field) we use the "floating mean" periodogram technique to estimate the characteristic variability timescale in each case. This method works better than the traditional Lomb-Scargle algorithm (Lomb 1976; Scargle 1982) for small number of points and has been successfully applied to planet searches (Cumming, Marcy & Butler 1999) and to determine the orbits of subdwarf B binaries (Morales-Rueda et al. 2003). A minimum number of 5 V measurements is required to calculate the floating mean periodogram.

The floating mean periodogram consists of fitting the data with a model composed of a sinusoid plus a constant of the form:

$$A(t) = \gamma + K \sin(2\pi(t - t_0)/P),$$

where γ is the average V magnitude, K is the amplitude of the V variability, P is the period and t is the time of observation. For each given period we perform singular value decomposition least square fitting of the data solving for γ

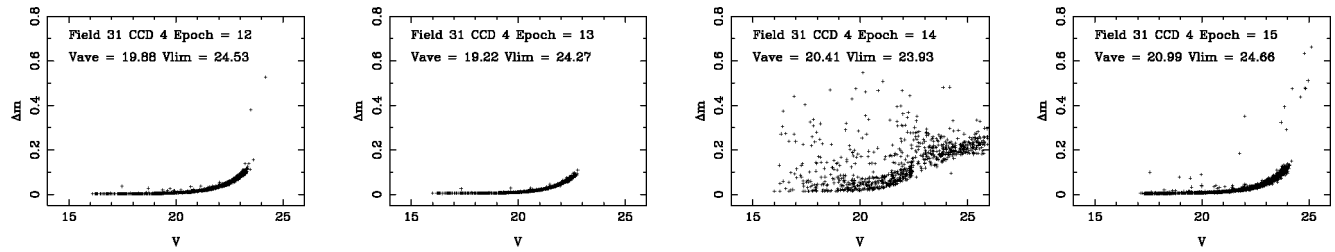

Figure 1. V magnitude versus V error for each point source detected in Field 31 CCD 4 in 4 different epochs. These plots were generated for all fields to check the quality of the data. See text for details.

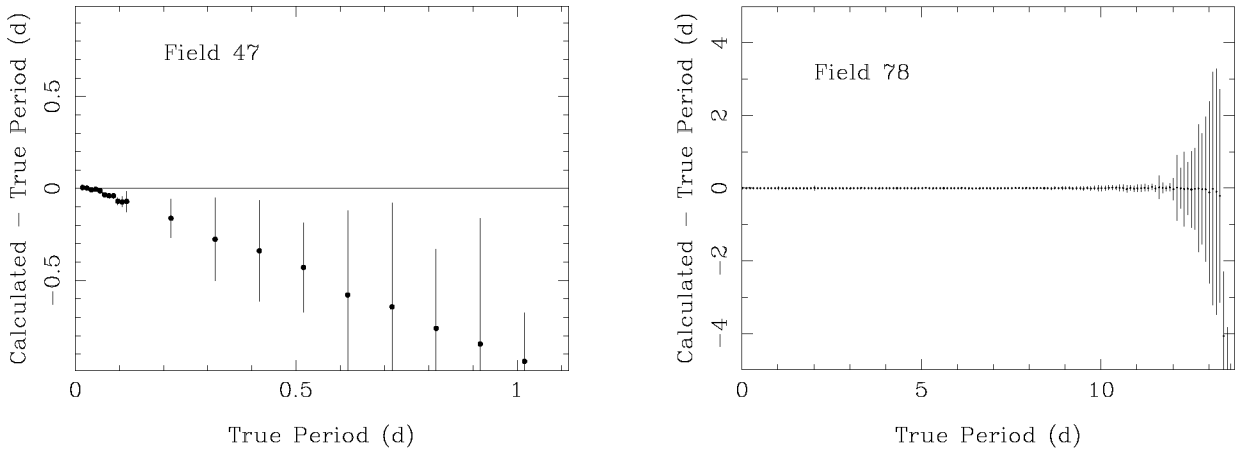

Figure 2. True period versus calculated-true period using the floating mean periodogram for two example fields, 47 with 5 V band measurements and 78 with 33 measurements. The period search was stopped when either the difference between the calculated and the true period was larger than 3× the error in the period, or the maximum searchable period was reached, i.e. 2× time baseline (although this last condition was never reached). The ratio of the amplitude of the variability to error assumed in both examples is 50.

and K (Press et al. 1992). We obtain the χ^2 of the fits as a function of frequency $f = 1/P$ and select the minima of this χ^2 function.

To test whether the periodogram was able to recover the correct periods we generated, for at least 9 different amplitudes per field, synthetic lightcurves that vary sinusoidally with periods between 24 min and several days (we chose the upper limit to be twice the time span of the observations) in period steps of 0.1 days, using the time sampling of each field. For each amplitude and period, we generated lightcurves with 20 different phasings, i.e. 20 different t_0. For each of these 20 phasings, we generated 10 lightcurves where the magnitude for each point was calculated given the period, the phasing, the amplitude and a fixed average magnitude. An error was added to the resulting magnitude for each point. This error was calculated by drawing a random number from a normal distribution centred on zero with standard deviation of 0.03, which is the average V band error found in the FSVS data.

We then used the floating mean periodogram to calculate the most probable period for each lightcurve, averaging the periods obtained for the 200 different lightcurves generated for each input timescale and amplitude. The average obtained was a weighted average where the weights used were the errors of the periods determined. We stopped the period search when the difference between the true and the calculated period was larger than 3σ. This condition was always reached before we got to the maximum period allowed in the search. We noticed large deviations (although still within the 3σ difference) between the calculated and true values at certain isolated periods. In these cases the true value for the following periods was again successfully recovered. These deviations are caused by the sampling windows of each given field. The presence of these isolated deviations prompted us to select the criteria described above to stop the simulated lightcurve fitting even when, in occasions, the errors on the calculated period were so large as to render the period determination highly inaccurate. To account for this inaccuracy, we will apply further filtering criteria to the errors of the periods determined from the data in Section 4.3.

After carrying out the simulations, the result for each field, or at least for the ones with more than 10 observations, is that true periods are recovered successfully with an error that increases with period. A few fields also show small deviations (but still within 3σ) from the true values at the shortest period (24 min). A common trend we observe is that, as we are reaching the limit period, the calculated values tend to underestimate the true periods at the same time that the error in the calculated period increases. This is clear in both panels of Fig. 2 where we have plotted the calculated period

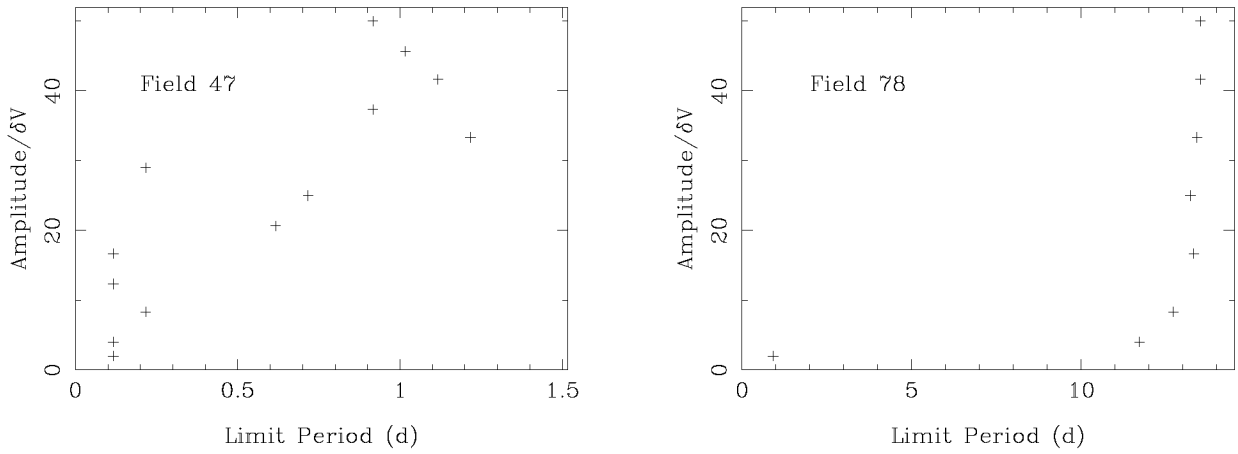

Figure 3. Maximum period that can be reconstructed from the simulated data depending on the ratio of the amplitude of the variability and the error in V (δV). The period search was stopped when the same conditions described in Fig.2 were reached. The period search was carried out fixing the error in V to 0.03 mags and changing the amplitude of the variability. This is the average error in brightness we find in the FSVS.

versus the true period. This seems to indicate that, when pushed to the limit, the periods calculated by the floating mean periodogram will be shorter than the true ones. Fig. 2 shows, as an illustration, two example graphs for two fields that have a very different number of observations, field 47 with only 5 V band observations and field 78 with 33 observations. Notice that not only the number of observations is of importance, but that using a different time sampling also generates slightly different graphs even with the same number of observations. The amplitude of the variability assumed also influences indirectly the maximum period we can determine in each case. Specifically, it is the ratio between the amplitude of the variability and the errors in the photometry which influence the success in recovering a period. By fixing the photometric errors in the simulations to $\sigma_{\rm average} = 0.03$ mag, we explore the influence of this ratio by varying only the amplitude of the variability. The graphs in Fig. 2 have been obtained assuming a variability amplitude of 1.5 mags (the maximum value used in the simulations) equivalent to an amplitude - V band error ratio of 50.

We obtain similar curves for all the fields to determine how effective the algorithm is at finding the true periods depending not only on the sampling and the number of observations, but also on the amplitude of the variability and the brightness of the objects (which define the errors in the V band magnitudes). For each field we generate a curve like those shown in Fig. 3, which present the maximum period that we can reconstruct from the simulated data for a range of variability amplitudes. As expected, the larger the amplitude of the variability (equivalent to a larger amplitude-error ratio), the longer the timescale of the variability that we can detect. The sampling and the time span of the observations have a direct influence on the maximum period we can detect. The graphs are presented only for the two example fields, 47 and 78, where the number of V band observations is very different over the same time span, $\sim$7 d. In the case of field 47, with only 5 measurements, the maximum period we can reconstruct before the difference between true and calculated period is larger than 3σ is about 0.4 d (see left panel of Fig. 2). Its limit period graph (left panel of Fig. 3) shows some departures from the expected behaviour, i.e. higher limit period as the amplitude/error ratio increases. In contrast, for field 78, with 33 V measurements we can detect periods of up to 13.5 d for the same variability amplitude and the limit period graph shows the expected behaviour. A similar number of measurements over a shorter time span will only allow us to measure shorter variability timescales. E.g. for field 26, with 29 measurements over 5 d, the maximum period we can reconstruct (for variability amplitude of 1.5 mags) is 9.3 d.

We want to remind the reader at this point, that by using the floating mean periodogram we are fitting the data with sinusoidal curves. Any non-sinusoidal, or indeed any non-periodic variability present in the data will be poorly fitted.

The maximum period that can be reconstructed for all the fields in the FSVS simultaneously is plotted in Fig. 4. For an amplitude of the variability of $\sim$0.25 mags (equivalent to an amplitude to magnitude error ratio of $\sim$8.3), we can reconstruct variability periods of up to 1 d for $\sim$17.58 deg^2 out of the 18.11 deg^2 available for search (66 fields out of the 68 with more than 4 V band measurements), we can reconstruct variabilities of up to 5 d for $\sim$13.31 deg^2 (50 fields). For amplitudes of 1.5 mag (magnitude error ratio of 50) we can reconstruct periods of up to 11 days for a region of 6.66 deg^2 (25 fields) and so on. We can only search for periods of the order of 20 days in 2 fields.

We are also interested in detecting small amplitude and short period variability, the limits of the data being a 24 min sampling and the photometric accuracy of $\sim$3 millimags for the brightest objects (Groot et al. 2003). The right panel of Fig. 4 zooms into the the short timescale, small amplitude variability region. We reconstruct successfully (i.e. with less than a 3σ difference between the true and calculated period) the minimum searchable period in all fields.

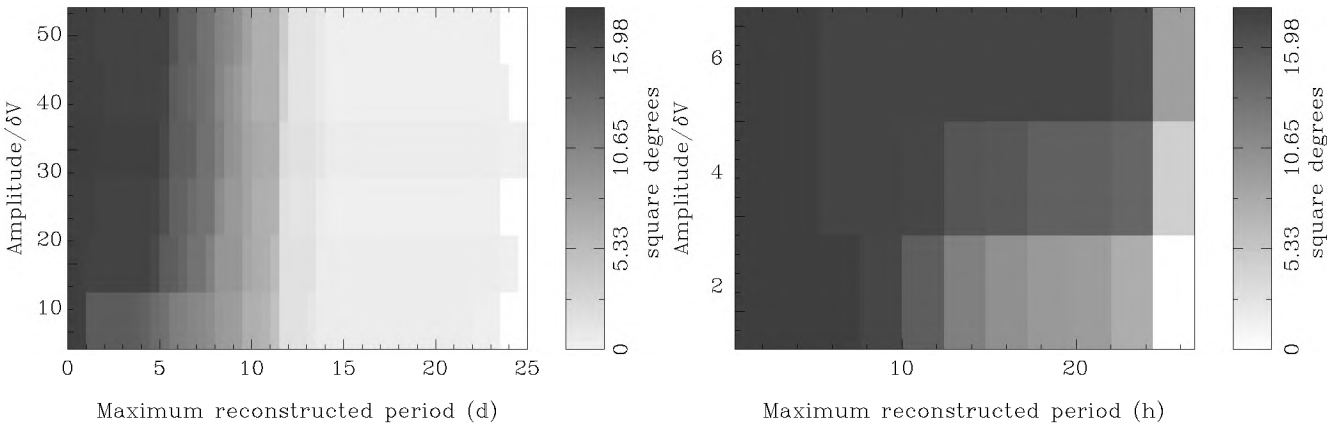

Figure 4. Left panel: gray scale map presenting the number of deg^2 in the sky for which we can reconstruct a given variability timescale depending on the ratio of the variability amplitude and the magnitude error. Note that if a variability scale of 5 days can be reconstructed for a given field also variabilities smaller than 5 days can be reconstructed. The minimum limit being the minimum possible searchable period of 24 min. Right panel: same information but zooming into the short period, small amplitude/error region. We reconstruct the minimum searchable period for all fields. Note that the structure seen on this panel cannot be seen on the left hand side panel due to the coarser binning in Amplitude/δV of the left hand side panel.

3.2.1 Our efficiency to detect the variability timescales of some interesting astronomical objects

Some interesting astronomical objects such as Cataclysmic Variables (CVs) and RR Lyr show characteristic variability timescales. CV periods range from 80 min to ∼6 h (although some of them show longer orbital periods such as GK Per with a 2 d orbit). The variability of RR Lyrae ranges from ∼6 h to about 1 d. Other interesting systems such as AM CVn binaries show orbital periods of the order of tens of minutes, too short to be detected in the FSVS. On the other hand, orbital periods of 80 min will be detected in the full area of the FSVS, as long as the ratio of the amplitude of the variability and the error in the V magnitude is at least 10, i.e. we would be able to detect all 80 min variables down to V = 24 if their variability amplitude is at least 2 mag, down to V = 23 if the variability amplitude is at least 0.7 mag, and down to V = 22 if the variability amplitude is at least 0.36 mag. CVs show characteristic orbital variability amplitudes of the order of 0.1–0.4 mag thus we will be able to detect a fraction at least down to V = 22. For certain fields, when looking at the short period region, the calculated period underestimates the value of the true period. This will most probably happen also for the real lightcurves.

Orbital periods of up to 6 hours, and between 6 hours and 1 day (this last period range is typical of RR Lyr) will be detected in 17.58 deg^2 (all fields but two) as long as the ratio of the amplitude of the variability and the V error is at least 20, i.e. we would be able to detect all variables with periods of up to 1 day in this area down to V = 24 if the variability amplitude is larger than 4 mag, and down to V = 23 if the variability amplitude is at least 1.4 mag. The variability amplitudes typical of RR Lyr range between ∼0.5 and >1 mag, which indicates that we are sensitive to RR Lyr down to V = 23 as long as the variability amplitude is at least ∼1.4 mag.

Other pulsating stars such as γ Doradus stars, δ Scuti stars, slowly pulsating B stars, β Cep stars and short period Cepheids show pulsation periods and amplitudes in the detectable range of this survey. Some of them, like δ Scuti stars, show very complicated oscillation patterns that are far from sinusoidal which means that, although they would be detected as variables with the χ^2 test, the periods reconstructed with the floating mean periodogram will most probably be incorrect. Short period pulsators such as rapidly oscillating Ap stars, PG1159 stars, pulsating subdwarf B stars and pulsating white dwarfs, and long period pulsators such as RV Tauri stars and Mira stars will not be detected in the FSVS as their pulsating periods lie outside the range we are sensitive to. Solar-like stars show very small amplitude pulsations that cannot be detected in the FSVS.

Asteroids show rotational periods of the order of a few hours and also lie in the detectable range of the FSVS. We see a number of asteriod tracks in the FSVS images but these asteroids do not stay in the same position from image to image and are discarded during data reduction.

We will use these results again in Section 4.3 to estimate how reliable our detections and non-detections for variability are at given timescales and amplitudes.

4 RESULTS

4.1 Fraction of variable sources

In the entire FSVS, using the χ^2 test, after discarding problematic points, we find a total of 1 713 short timescale variable V-band point sources that have been detected also in the B and I bands. The number of non variable sources found (after applying the same criteria as for the variables sources, i.e. account for problematic points and positive detections in B and I) is 173 276 (∼1 percent of all point sources detected are short term variables).

In the top left panel of Fig. 5 we present the distribution of sources in the FSVS in the form of a grey-scale plot, which shows that most objects fall along the main sequence with the largest numbers at its blue end. The top right panel presents the same plot for the variable sources in the FSVS

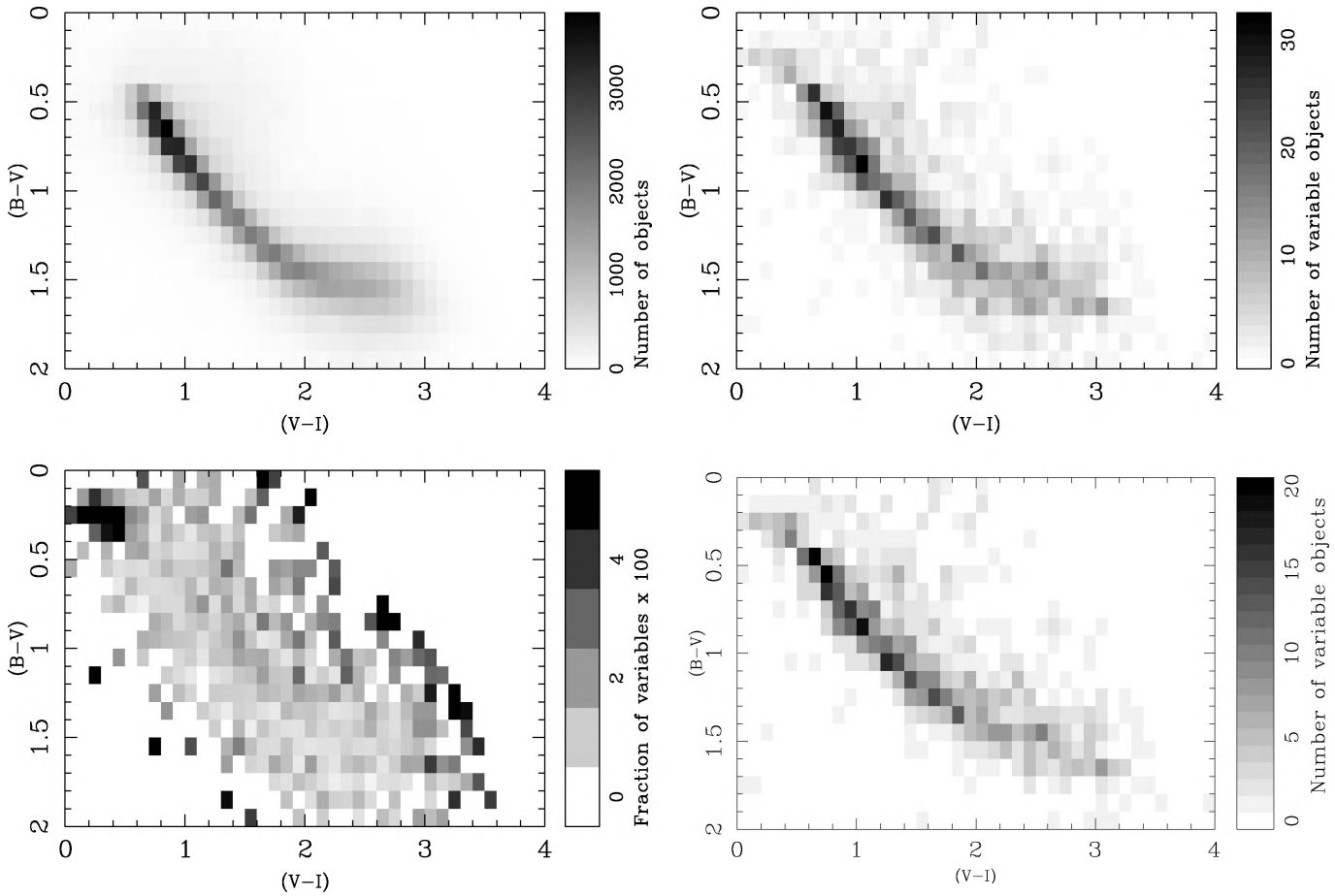

Figure 5. Top left panel: non variable sources in the FSVS. Top right panel: short term variable sources in the FSVS. Bottom left panel: fraction of short term variable sources in the FSVS. The fraction is presented in percentages. The region in the colour-colour diagram where there are more variable sources lies above the blue cut-off, i.e. (B−V)<0.38, and 0<(V−I)<1. Bottom right panel: colour-colour diagram presenting the 976 variable point sources that have more than 4 measurements and can be studied using the floating mean periodogram method. Note that some of the blue variables found in this diagram might be QSOs.

as determined by the χ^2 test. Again, most sources are situated along the main sequence, but there is also a significant fraction of sources above the main sequence and as a 'blue' extension of the main-sequence. To highlight the difference in distribution between the variable and non variable sources we present the fraction of variable sources as a function of colour in the lower left panel (which is basically the ratio of the upper two panels in Fig. 5). This shows a clear enhancement of sources above the blue tip of the main sequence (about 4 percent are variable) and a less marked enhancement to the right and above the main sequence while the main sequence itself appears as an area with relatively few variables, of the order of 1 per cent. These values agree with those found by Everett et al. (2002) in a similar, albeit shallower, study.

The fraction of variable point sources found in each field using the χ^2 test is given in Table 1. The fraction of variables differs from field to field ranging from 0.06 to 13.68 per cent. We find that fields with less than 4 measurements tend to have larger fractions of variables but we are not certain that there is a direct correlation with the number of observations and that other effects, such as position in the sky, are not taking place. If we do not consider the fields with less than 4 observations, we determine a 0.7 per cent fraction of variables in the full FSVS. The distribution along the main sequence decreases only slightly, by 0.2 per cent, for all colour-colour bins.

4.2 Sample of variables studied with the floating mean periodogram

Ten fields have less than 5 V measurements. The timescale of the variability for the variables in these 10 fields cannot be determined because of the low number of measurements, thus only a fraction of the 1 713 short term variables found in the FSVS can be studied in more detail using the floating mean periodogram. Once we account for fields with less than 5 measurements, for problematic epochs, and for objects that although observed more than 4 times, were only detected 4 times or less, we end up with 976 point sources that can be studied in further detail. In most cases the non detection of a source was the result of faint objects, occasionally falling below the limit of detection, and in some cases of the objects being blended or truncated. After ac-

Table 2. Fraction of variable objects (out of the 744) found in the FSVS for different cutoff limits on the error of the timescale and the error of the amplitude.

δP (%)	10	20	30	40
δA (%)				
10	29.4	29.7	29.7	29.7
20	75.7	76.2	76.3	76.3
30	91.4	92.2	92.6	92.6
40	96.6	97.4	97.8	97.8

counting for these three factors we find that the fraction of variable systems found is independent of the number of V measurements. For the objects with more than 4 detections, information about the timescale and amplitude of the variability can be obtained. The distribution of these 976 sources in the colour-colour diagram is given in the bottom right panel of Fig. 5.

4.3 Timescale and Amplitude of the variability

When we run the floating mean periodogram on the real data lightcurves we obtain their most likely variability timescale and the amplitude of the variability on that timescale. After rejecting those sources for which the period and amplitude measured lie outside the ranges that can be reconstructed, according to the simulations carried out in Section 3.2, we are left with 744 variable point sources out of the 976 mentioned above.

To understand this sample of variables, we select different cutoffs for the error in the variability timescale and amplitude calculated. Table 2 gives the fraction of variable point sources found for different combinations of error cutoffs in timescale and amplitude. Applying an error cutoff of 30 percent in the periods and 50 percent in the amplitudes we can already reconstruct the 744 initial variables. Applying an error cutoff of 30 percent in both period and amplitude we find that 50 percent of the variables show periods between 24 min and 6 hours, 22 percent between 6 hours and 1 day, 20 percent between 1 and 4 days, and 8 percent show periods above 4 days. If we apply fairly strict error cutoffs for the period and amplitudes, i.e. 10 percent, the number of variable sources decreases to 219, of which the distribution in the same period bins is 51, 20, 19 and 10 percent respectively.

If we assume a normal distribution for the data, a 50 percent error corresponds to 2σ, a 30 percent error to 3.3σ, a 20 percent to 5σ, and a 10 percent to 10σ.

The number of variable point sources for which we can determine their variability timescales and amplitudes by using the floating mean periodogram test is a very good fraction of the total number of variables detected using the χ^2 test (i.e. $\sim$700 out of the 976 if we use error cutoffs of the order of 30 per cent).

Fig. 6 shows the ratio of variable sources for which we have determined the timescale and the amplitude of their variability with an error less than 20 percent with the floating mean periodogram with respect to the number of sources flagged as variable with the χ^2 test as a function of the number of observations. To account for the fact that there

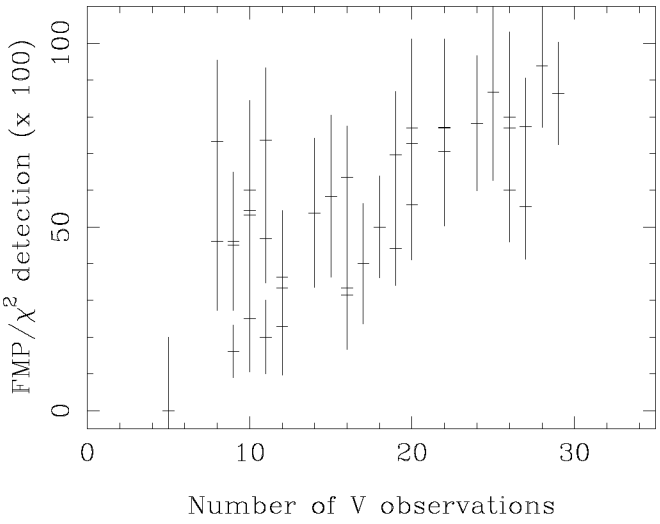

Figure 6. Ratio of variable sources solved with the floating mean periodogram with respect to the number of sources flagged as variable with the χ^2 test, as a function of number of observations. We have only included the sources determined using the floating mean periodogram that have errors of less than 20 percent. We only plot those fields that contain more than 10 variables. FMP stands for floating mean periodogram.

are large differences between the number of variable sources for each field, we have only plotted those fields for which the number of variable sources is 10 or more. There is a clear correlation between the number of observations and the fraction of variables we can solve with the floating mean periodogram. Including the fields with less than 10 variables increases the scatter in the plot, whereas including only those fields with 20 or more variables decreases the scatter. The slope of the correlation remains the same and indicates that with a number of observations of the order of 30, taken within a 2 week time span, we can reconstruct most variables present in the data (with those periods and amplitudes in the range determined in Section 3.2). Of course, this argument assumes that the lightcurves of the variables are close to sinusoidal.

Fig. 7 presents the distribution of variables we find in the FSVS according to the period and amplitude of the variability as well as their cumulative period distribution. The top panels consider the total number of variables in the trusted range of periods and amplitudes (689) where the error on the periods and amplitudes is less than 30 per cent. The bottom panels present the distributions when we only take the systems where the period and amplitude determined has a maximum error of 10 per cent. In both cases we find that most systems lie at short periods and low amplitudes, with only a few systems showing larger amplitudes and periods. We find that 50 per cent of the objects show periods below 6 hours with peaks in the 30 per cent error distribution at $\sim$24 min, $\sim$0.03 days ($\sim$43 min), $\sim$0.12 days ($\sim$2.9 hours), $\sim$0.79 days ($\sim$19 hours), $\sim$1.3 days and $\sim$4 days, and in the 10 per cent distribution at $\sim$0.12 days ($\sim$2.9 hours). In the 30 per cent period distribution, the clump of sources between $\sim$24 and 36 min ($-1.778 < logP < -1.6$) contains 67 sources. To confirm that these are short period variables, and not just a

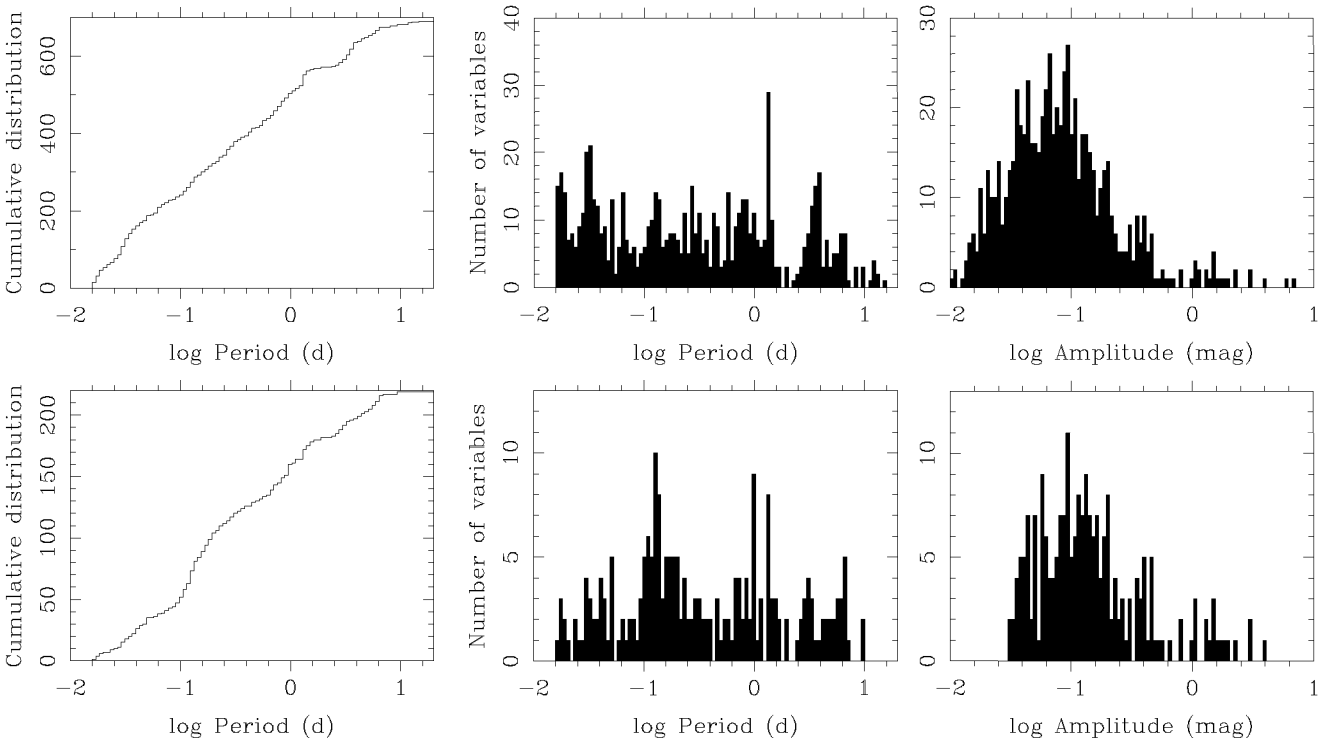

Figure 7. Histograms showing the cumulative period distribution (left panels), the period distribution (middle panels) and the amplitude distribution (right panels) for the short term variable point sources in the FSVS. Top: the 689 out of 744 sources with accuracies in the periods and amplitudes of the order of 30 per cent or less. Bottom panels: sources where the error in their periods and amplitudes is of the order of 10 per cent or less.

systematic problem caused by the sampling (after all the minimum period we are sensitive to is 24 min) they were inspected by eye resulting in 80 per cent being bona-fide short period variables with the remaining 20 per cent showing only one point off the average brightness of the target and thus giving the short period result based only on one point variability. These one point off sources are not present in the 10 per cent sample.

Regarding the amplitude distribution, 50 per cent of the objects show amplitudes lower than ∼0.07 mag in the 30 per cent error sample and lower than ∼0.12 mag in the 10 per cent sample.

When we combine the number of sources we find per period and amplitude bin with the sensitivity of the floating mean periodogram search, plotted in Fig. 4, we obtain lower limits for the space density of variables, i.e. number of variables per square degree, versus period. These are presented in the form of a histogram in Fig. 8. We see four distinct peaks in the distribution centred at 6 hours, 1 day, 3.75 days and 12.75 days with a somewhat less significant peak at 6 days. The highest density of variables show periods below 12 hours. These periods include CVs, RR Lyr stars, and other short period pulsators such as δ Scuti stars. The period range centred at 1 day includes also possible CVs, RR Lyr and other pulsators like γ Doradus stars and Pop II Cepheids. At 3.75 days we would still find some longer period CVs, γ Doradus stars, Pop II Cepheids and longer period pulsators such as subdwarf B stars. At periods around 12.75 days, we expect to find, apart from binaries with those

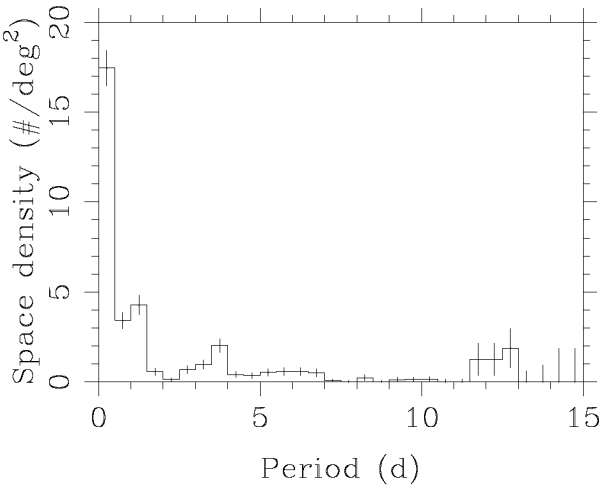

Figure 8. Space density of variables obtained from the FSVS.

orbital periods, Pop II Cepheids contributing to the space density of variables.

4.4 Variability colour-colour diagrams

Keeping in mind the uncertainty of the variability timescales determined, when we combine the variability information with the colour information available for the FSVS we obtain the colour-colour diagrams shown in Fig. 9. We find that, if we take only the sources with less than 30 per cent errors in their timescales and the amplitudes, 344 point sources

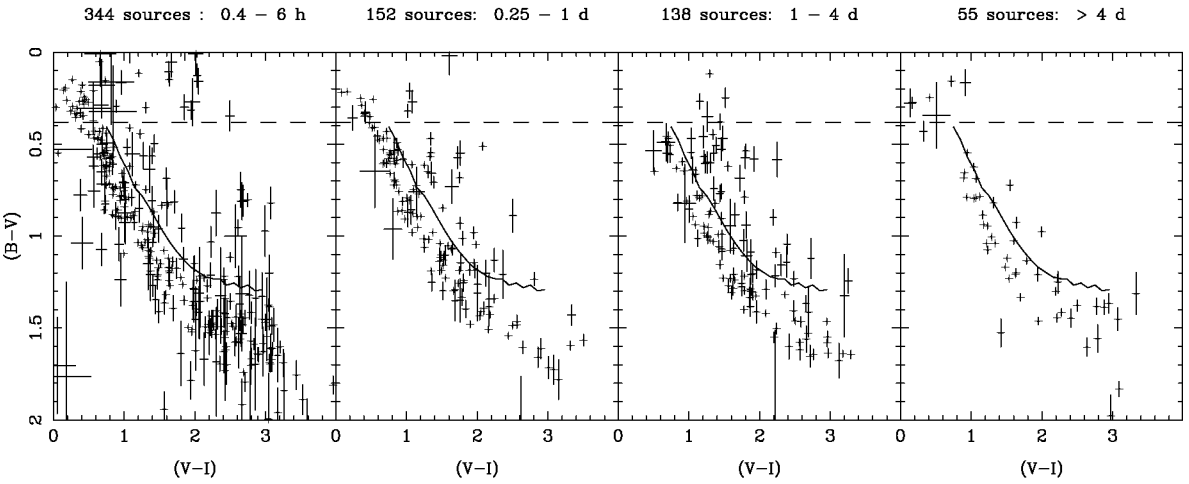

Figure 9. Colour-colour diagrams for several variability timescales obtained from the FSVS after applying a 30 per cent error cutoff in both the timescale and amplitude of the variability. The solid curve indicates the 3-σ upper limit of the main sequence. The dashed line indicates the blue cut-off at (B-V)<0.38.

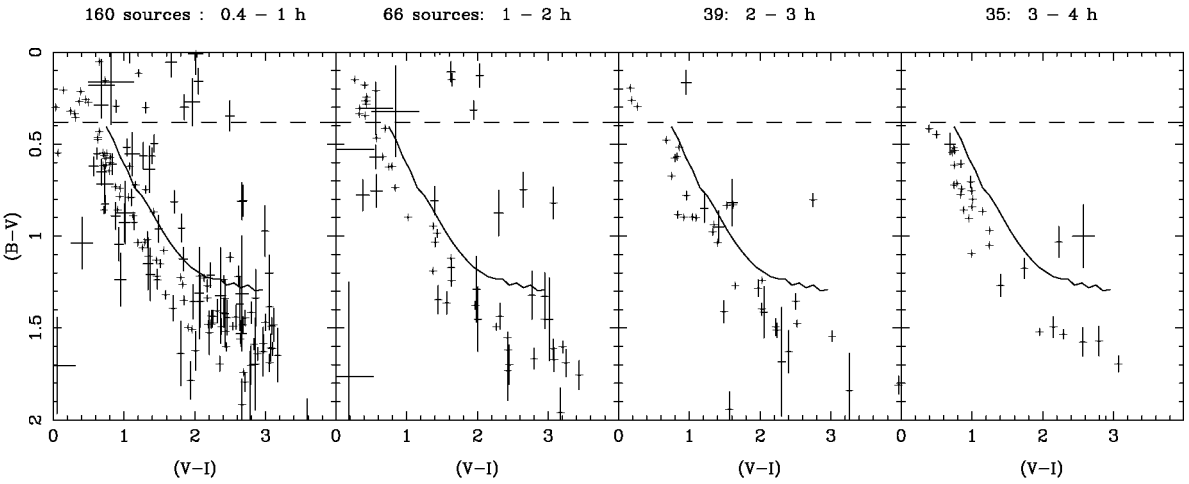

Figure 10. Same as in Fig.9 but only for short variability timescales. Most short period variables show variability timescales lower than 1 h.

show variabilities shorter than 6 h (0.25 days). These short timescale variables are found along the main sequence in the colour-colour diagram (see first panel of Fig. 9), where we expect to find for example δ Scuti stars, as well as above the main sequence and in more extreme colour areas usually filled by binary systems where one of the components is blue and the other red, e.g. detached red dwarf-white dwarf binaries. At these short timescale variabilities we also find a clump of objects above the, so called, blue cut-off at (B−V)<0.38. The blue cut-off of the main sequence results from the combination of the number density of different spectral types and the scale height of the Galaxy. The colours and the short variability timescales, of the order of characteristic close binary orbital periods, suggest that these sources above the blue cut-off are possibly interacting binary systems of the CV type or detached binary systems such as subdwarf B binaries. Longer coverage, better sampled lightcurves combined with spectroscopy are necessary in order to identify the sources.

The variable sources with timescales shorter than 6 h represent 50 per cent of the total number of short timescale variables in the survey. Fig. 10 shows how most of those short period sources subdivide in smaller variability timescale ranges. We find that about half of the short period sources have variability timescales shorter than 1 h. These are again distributed along the main sequence with a few objects placed above it.

There are 152 objects showing variability in the 0.25 - 1 d range. These objects are also mostly distributed along the main sequence, including γ Doradus pulsators amongst others, with some cases found in the extreme colour region. The RR Lyr variables present in the survey should be found in this variability range. If we combine this with the colours expected for RR Lyr systems, i.e. 0.1<(B−V)<0.45, 0.1<(V−I)<0.65 (Guldenschuh et al. 2005) we find 12 RR Lyr candidates. One of these will be discussed, as an example, in Section 4.6.

We find 138 sources that show variabilities between 1

and 4 d again distributed mostly along the main sequence. This would include γ Doradus pulsators as well as Pop II Cepheids. There are 55 point sources that show variabilities on timescales longer than 4 d. Binary systems with these periods as well as Pop II Cepheids are included in this period range. The blue sources found in these two period ranges above the blue cutoff could be subdwarf B slow pulsators or binaries.

Fig. 11 presents similar diagrams to those in Fig. 9 but for the sources where the error limits were set to 20 percent. The distribution of variables in the diagrams is very similar to the initial one. Again about half of the sources show variability timescales shorter than 6 h. Most of the objects that have disappeared from the diagram come from the shorter period ranges (23 per cent out of the 0.4 - 6 h bin and 22 per cent out of the 0.25 - 1 d bin). This could be due to the fact that if the signal is not sinusoidal or regular, the floating mean periodogram tends to calculate periods shorter than the input ones with large errors. It is worth noticing that a few of the interesting objects above the blue cut-off have disappeared.

4.5 Fraction of variable sources as a function of spectral type

The fraction of variable point sources along the main sequence, as a function of spectral type (as defined in Johnson 1966), is presented in Table 3. The number of variables used here is that obtained from the χ^2 test. The fraction of variables is constant with spectral type and has a value around 1 per cent.

We also present the distribution of variability periods and amplitudes measured for the number of variables that were analysed with the floating mean periodogram algorithm. Four period bins and four amplitude bins are presented in Table 4. Some spectral type ranges contain very few objects. For those with a larger number of objects (K0 to M5) the variable sources spread themselves in similar fractions in the spectra ranges K0 to M0 with more short period systems in the spectral range M0 – M5. The fraction of variables with timescales longer than 4 days is significantly smaller than in the other timescale bins. In the case of the amplitudes of the variability, most sources show variabilities with amplitudes lower than 0.1 mags.

4.6 Example lightcurves

Fig. 12 presents the lightcurves for two example sources found in our data. The examples have only been selected to illustrate two very different samplings. The first example corresponds to one of the candidate RR Lyr (see Section 4.4) for which we determined a period of 6.34 h from the floating mean periodogram. The second example corresponds to a source with very blue colours, for which we have obtained spectra that suggests it is a subdwarf B star. The period measured for this system, which probably corresponds to its orbital period in a binary system, is 4.95 h. For both sources we present the measurements as a function of phase folded at the period determined from the floating mean periodogram. The best sinusoidal fit to the data is also plotted.

The FSVS covers a region in the sky in which there are two known cataclysmic variables, GO Com and V394 Lyr. These two sources were identified as variables in both the χ^2 and the floating mean periodogram tests. Interestingly enough, both of them went into outburst during the observations which made it more difficult to determine their orbital periods. GO Com was observed in three different epochs and it rose by a magnitude in V from the second to the third epoch (from 19.4 to 18.5). In an attempt to subtract the outburst contribution to the variability, and thus to be able to measure its orbital period, we calculated its average brightness for each epoch and subtracted the average from the measurements taken on that epoch. When we run the floating mean periodogram on the resulting lightcurve we obtain a periodogram with two main groups of aliases, one centred in 30 min and another on 90 min. The sampling of the lightcurve does not allow us to determine the period with more accuracy than this. The second alias lies near the 94.8 min period determined by Howell et al. (1995). V394 Lyr was observed in 7 epochs and it rose by two magnitudes in V from the first to the sixth (from 19.1 to 17) starting to decrease on the the seventh. We followed the same steps outlined above for GO Com and found the lower χ^2 aliases to be 43 min and 4.32 h. There are no measurements of the orbital period of V394 Lyr in the literature that we can compare these values with. The folded lightcurves on these two periods do not look convincing which lead us to think that none of these are the true orbital period of the system.

4.7 Sources not detected in all three bands

A third of the variable point sources found in the FSVS using the χ^2 test were not detected either in B, I or in both B and I bands. In a handful of cases this was due to the point source being close to the CCD boundary, in 21 percent of the cases the source appeared as blended with another one, in 28 per cent of the cases the source was not detected because it was too faint, and in 50 per cent of the cases the source was saturated in the I band. Most of these sources saturated in the I band are very bright in the three bands (71 percent) indicating that about one sixth of the variable sources found are at the bright end of the survey. This is expected as most variables probably show low amplitude variations which are easier to detect for bright sources. In the case of the blended sources, blending would most probably affect the V band magnitudes perhaps introducing spurious variability.

On the other hand, 29 percent of the sources undetected in B and/or I, do show larger colour differences, (B−I)>3 and up to 5 magnitudes in some cases. Colour differences of (B−I)>3 are expected for some main sequence stars and do not imply that we are dealing with extreme colour objects. The lower limit colours calculated for these sources (by assuming their I band magnitude is equivalent to the I band magnitude of the brightest unsaturated star in the field) fill an area of the colour space, which is also filled by the point sources that were detected (unsaturated) in the three bands. This indicates that, although their colours are more extreme, they are not unusual compared with the sources detected in all three bands, they are just brighter and therefore saturated in the I band.

The same analysis carried out in Section 4.3 for point sources with B, I and V detections, and more than 4 V

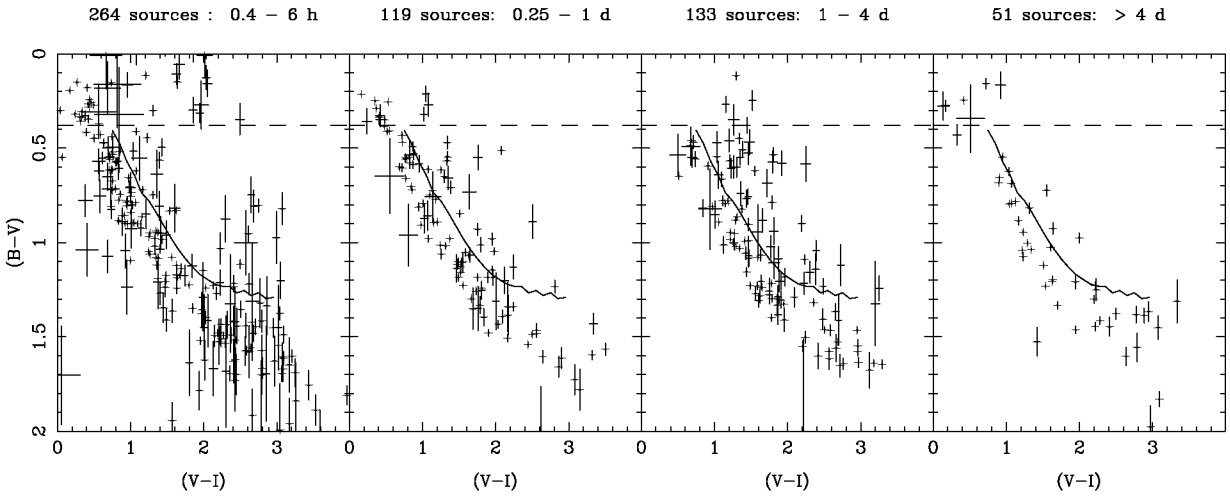

Figure 11. Same as in Fig.9 but with error limits set to 20 for both timescales and amplitudes.

Table 3. Fraction of variable sources per spectral type bin found in the FSVS. Notice that although the first main sequence bin (spectral types F0–F5) contains more variables than the rest, this is likely to be the result of including non main sequence sources in that bin. Non MS stands for non main sequence sources. Two fractions are given, for all sources in the FSVS and only for those with more than 3 V measurements.

Spectral type	B−V	V−I	# Var	# Sources	Fraction (%)
non MS	< 0.38	0.47–0.64	11	700	1.6
non MS	< 0.38	0.00–0.4	29	833	3.5
F0–F5	0.31–0.43	0.47–0.64	13	602	2.2
F5–G0	0.43–0.59	0.64–0.81	62	6054	1.0
G0–G5	0.59–0.66	0.81–0.89	20	1816	1.1
G5–K0	0.66–0.82	0.89–1.06	63	6814	0.9
K0–K5	0.82–1.15	1.06–1.62	204	20207	1.0
K5–M0	1.15–1.41	1.62–2.19	133	12974	1.0
M0–M5	1.41–1.61	2.19–3.47	153	16256	0.95
M5–M8	1.61–2.00	3.47–4.70	3	179	1.7

measurements can be carried out for 154 sources with no B and/or I detections. In these cases the information we have of the variable sources is only their timescales and amplitudes and not their colours. Once we discard sources for which their calculated periods and amplitudes lie outside the trustable ranges determined in Section 3.2 for each field, we are left with 71 short period variable sources. We find that 29.5 per cent of the variables with 30 per cent accuracy in their periods and amplitudes show periods between 0.4 and 6 hours, 39.3 per cent between 6 hours and 1 day, 21.3 per cent between 1 and 4 days, and 9.8 per cent of more than 4 days. These values are slightly different (19, 23.8, 33.3 and 23.8 respectively) if we consider the 21 sources where the periods and amplitudes determined have errors of less than 10 per cent. When we compare this distribution of variables in period bins with the one we found for systems with B and I measurements (50, 22 20, 8 per cent respectively for each period bin), we find that the number of shorter period variables (first period range) is smaller for the sources with no B and/or I detections and the number of variables in the last two period bins is larger.

5 CONCLUSIONS

We have analysed the short timescale variability information contained in the FSVS and find that about 1 per cent of all point sources are variable. Of those variables, about 50 per cent show variability timescales shorter than 6 hours, 22 per cent show variabilities between 6 hours and 1 day, 20 per cent between 1 and 4 days and 8 per cent show periods longer than 4 days. The distribution of variables with spectral type is fairly constant along the main sequence, with 1 per cent of all the sources being variable, except at the blue end of the main sequence where the fraction of variable sources increases possibly due to contamination by non main sequence sources. Above the main sequence, beyond the blue cut-off at (B−V)<0.38, we find that the fraction of variables increases to 3.5 percent.

The highest space density of variables found in the FSVS (i.e. 17 per deg^2) show periods below 12 hours. These include CVs, RR Lyr stars, and other short period pulsators such as δ Scuti stars. We find a density of 4 variables per deg^2 centred at a 1 day period which includes longer period CVs, RR Lyr and other pulsators like γ Doradus stars and Pop II Cepheids. A space density of 2 variables per deg^2 at 3.75

Table 4. Period and amplitude distribution of the main sequence variables analysed with the floating mean periodogram. Four bins for the variability timescale and four for the variability amplitude are shown. The percentage of sources in each bin is given. FMP stands for floating mean periodogram. Amplitudes are given in magnitudes.

Spectral type	# VarFMP	Period distribution(%)				Amplitude distribution(%)			
		0.4–0.6 h	0.25–1.0 d	1.0–4.0 d	>4 d	0.01–0.1	0.1–0.25	0.25–1.0	>1.0
F0–F5	6	50.0	33.3	0	16.6	16.6	50.0	16.6	16.6
F5–G0	30	53.3	23.3	23.3	0	60	26.6	10.0	3.3
G0–G5	6	50.0	33.3	16.6	0	83.3	16.6	0	0
G5–K0	18	61.1	22.2	5.5	11.1	88.8	11.1	0	0
K0–K5	86	43.0	23.2	23.2	10.5	82.6	11.6	5.8	0
K5–M0	66	36.4	33.3	25.8	4.5	77.3	12.1	7.6	3.0
M0–M5	69	63.8	10.1	18.8	7.2	78.3	17.4	4.3	0
M5–M8	2	100.0	0	0	0	50	50	0	0

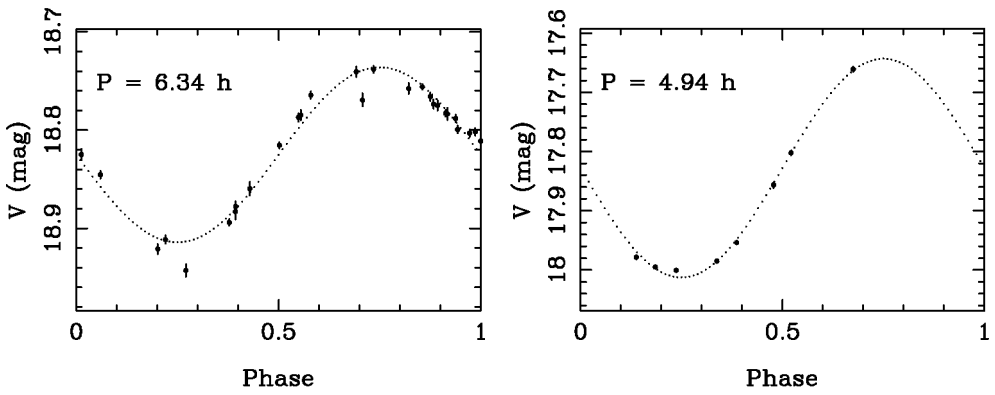

Figure 12. Lightcurves of two example objects folded on the period determined with the floating mean periodogram. The left hand side lightcurve corresponds to one of the RR Lyr candidates discussed in Section 4.4 and the right hand side lightcurve to a subdwarf B star candidate. The best sinusoidal fit is also plotted.

days includes, some longer period CVs, γ Doradus stars, Pop II Cepheids and longer period pulsators such as subdwarf B stars. At 12.75 days we also find 2 variables per deg^2. These would be mainly binaries with those orbital periods and Pop II Cepheids.

It is easier to compare these space densities with those expected for the mentioned populations when we combine the period information with the colours of the populations under study. The case of CVs and many pulsators is complicated as they appear mixed through several period and colour ranges and in many cases it is necessary to obtain spectra to confirm the nature of the variable source. The space densities of CVs and subdwarf B stars will be studied in detail in a future paper. In the case of RR Lyr stars, we find 3 certain members and 9 other candidates down to V = 21.6. Assuming we have detected all RR Lyr between V = 16–22, we determine a space density of $\sim 10^{-3}$kpc^{-3} in agreement with the space density determined by Preston, Shectman & Beers (1991) at a distance of 100–150kpc from the Galactic Centre.

By using the floating mean periodogram, we have determined the most likely periods and amplitudes of a fraction of the variables found in the FSVS. We find that we are complete down to V = 22 for CVs in the minimum period (80 min) as long as they show variability amplitudes of the order of 0.4 mag. We are complete down to V = 22 for periods between 80 min and 1 day in a 17.82 deg^2 area of the survey as long as the amplitude of the variability is at least 0.7 mag. This includes most RR Lyr stars. We will be able to detect RR Lyr also down to V = 23 when their variability amplitudes are at least 1.5 mag.

ACKNOWLEDGEMENTS

We thank T. R. Marsh for making his analysis software available. The FSVS was supported by NWO Spinoza grant 08-0 to E. van den Heuvel. The FSVS is part of the INT Wide Field Survey. LM-R, PJG and EvdB are supported by NWO-VIDI grant 39.042.201 to PJG. GN is supported by NWO-VENI grant 639.041.405. The Isaac Newton telescope is operated on the island of La Palma by the Isaac Newton Group in the Spanish Observatorio del Roque de los Muchachos of the Instituto de Astrofísica de Canarias.

REFERENCES

Becker, A. C., et al., 2004, ApJ, 610, 679
Brinkworth, C. S., Marsh, T. R., Morales-Rueda, L., Maxted, P. F. L., Burleigh, M. R., Good, S. A., 2005, MNRAS, 357, 333

Brown, T. M., Gilliland, R. L., 1994, ARA&A, 32, 37
Cumming, A., Marcy, G. W., Butler, R. P., 1999, ApJ 526, 890
Downes, R. A, Webbink, R. F., Shara, M. M., 1997, PASP, 109, 345
Everett, M. E., Howell, S. B., van Belle, G. T., Ciardi, D. R., 2002, PASP, 114, 656
Groot, P. J., et al., 2003, MNRAS, 339, 427
Guldenschuh, K. A. et al., 2005, PASP, 117, 721
Howell, S. B., Szkody, P., Cannizzo, J. K., 1995, ApJ, 439, 337
Huber, M. E., Everett, M. E., Howell, S. B., AJ, 2006, in press
Johnson, H. L., 1966, Ann. Rev. Astron. Astro. 4, 193
Lomb, N. R., 1976, Ap&SS, 39, 447
Morales-Rueda, L., et al., 2003, MNRAS, 338, 752
Press, W. H., Teukolsky, S. A, Vetterling, W. T., Flannery B. P., 1992, Numerical recipes in C: The art of scientific computing, Cambridge University Press
Preston, G. W., Shectman, S. A., Beers, T. C, 1991, ApJ, 375, 121
Ramsay, G., Hakala, P., 2005, MNRAS, 360, 314
Scargle, J. D., 1982, ApJ, 263, 835
Street, R. A. et al., 2005, MNRAS, 358, 795
Tyson, J. A., 2002, Proceedings of the SPIE, 4836, 10